

Size-dependent fivefold and icosahedral symmetry in silver clusters

Xiaopeng Xing,¹ Ryan M. Danell,¹ Ignacio L. Garzón,² Karo Michaelian,² Martine N. Blom,³ Michael M. Burns,¹ and Joel H. Parks^{1,*}

¹Rowland Institute at Harvard, 100 Edwin H. Land Boulevard, Cambridge, Massachusetts 02142, USA

²Instituto de Física, Universidad Nacional Autónoma de México, A.P. 20-364, 01000 Mexico, DF, Mexico

³Institut für Nanotechnologie, Forschungszentrum Karlsruhe, Postfach 3640, 76021 Karlsruhe, Germany

(Received 17 June 2005; published 23 August 2005)

Trapped ion electron diffraction measurements on silver cluster cations, Ag_n^+ for sizes $n=36-46,55$ at ~ 120 K describe an evolution in structural symmetry with increasing cluster size. Diffraction patterns characterize fivefold symmetry at smaller sizes which evolves to icosahedral symmetry at $n=55$. Low energy isomer structures were identified by statistical search methods and optimized by density-functional calculations. Comparison of diffraction data with these theoretical structures confirms the presence of local order having fivefold symmetry for sizes $n=36-39,43$ and global order having icosahedral symmetry at the closed shell size $n=55$.

DOI: 10.1103/PhysRevB.72.081405

PACS number(s): 61.14.-x, 36.40.Mr, 61.43.-j, 64.70.Nd

The study of small metal clusters has made extensive contributions to understanding the size-dependent, many-body character of nanoscale physics and chemistry. Important examples which have increased our appreciation of the different forms in which size dependence is manifest include measurements and calculations of metal cluster melting,^{1,2} the transition of planar to three-dimensional structures,^{3,4} and the reactivity of gold cluster nanocatalysts.^{5,6} This paper presents measurements of the structure of mass selected metal clusters by trapped ion electron diffraction. Diffraction techniques have been shown to be particularly sensitive to the measurement of size-dependent changes in structural symmetry for small clusters.⁷ Measurements presented here investigate the development of silver cluster structures over the size range 36 to 55 atoms to develop an understanding of how cluster structures evolve through intermediate sizes to achieve “magic number” structures composed of closed electronic or atomic shells. These measurements⁸ have discovered an evolution from short-range order among nearest neighbors having fivefold symmetry to a global order having icosahedral symmetry at $n=55$. The local fivefold symmetry does not result from the decoration of an inner icosahedral core of 13 atoms having icosahedral (Ih) symmetry. Not a single isomer calculated for cluster sizes below $n=55$, comprising a total of ~ 40 density functional theory (DFT) optimized cluster structures, contains an icosahedral core. The local order in these calculated structures becomes apparent only after an order analysis of the cluster structure.

The trapped ion electron diffraction apparatus⁹ has been greatly modified for these experiments, the details of which will be published elsewhere. The metal cluster source includes a liquid nitrogen cooled aggregation tube enclosing a magnetron sputter discharge similar to that designed by the Haberland group.¹⁰ The cluster ion beam emitted by the source enters an electrostatic quadrupole bender which directs the beam either to a time-of-flight mass spectrometer or to the diffraction beamline. The beam enters a second smaller quadrupole bender which directs the ions to an aperture in the rf trap endcap electrode. The trap stores $\sim 5-8 \times 10^3$ mass selected cluster ions which are collision-

ally relaxed to the temperature of the trap and He background gas of ~ 120 K. To ensure that trapped clusters are as close as possible to an equilibrium distribution, clusters can be annealed by applying an external rf field resonant with the ion motion frequency to heat clusters by translational to vibrational (T-V) transfer in collisions with a background Ne gas. This annealing step was only recently introduced and applied here to a few cluster sizes to investigate the possibility of kinetic effects during cluster formation. After annealing, the cluster ensemble is cooled to the He gas temperature over $\sim 3-5$ s. Clusters prepared in this way minimize the effects of source parameters on the measured cluster structure. In a typical experimental run over $\sim 4-5$ h, the diffraction pattern is an average over $\sim 1-3 \times 10^6$ mass selected clusters.

The total scattering data for all sizes studied are displayed in Fig. 1. The inset of Fig. 1 shows the total charge-coupled device (CCD) image of Ag_{55}^+ . The total scattering plots are an integration of the CCD pixel intensity about ring image center. The pixel distance corresponding to the scattering momentum transfer, s , is fit during comparison with theory. The momentum transfer is related to the scattering angle, θ , by $s=(4\pi/\lambda)\sin(\theta/2)$ where $\lambda=0.06$ Å is the de Broglie wavelength for 40 keV electron energy. The total scattering intensity, I_{total} , in the range $s \approx 3.5-4$ Å⁻¹ changes with cluster size although the overall characteristics are very similar. These changes will be shown to be related to the evolution from local order having fivefold symmetry to global order having icosahedral symmetry at Ag_{55}^+ . The total scattering is approximated by the sum of independent scattering terms, I_{indep} , from each cluster atom and terms resulting from the interference of elastic scattering from pairs of atoms. Multiple scattering does not contribute significantly for clusters in this size range.

The data analysis extracts the interference or molecular scattering intensity from the total scattering by approximating the independent scattering contribution by a 4th order polynomial in s . The resulting molecular scattering intensity, defined by $sM(s)=s(I_{\text{total}}-I_{\text{indep}})/f^2$, where f is the atomic

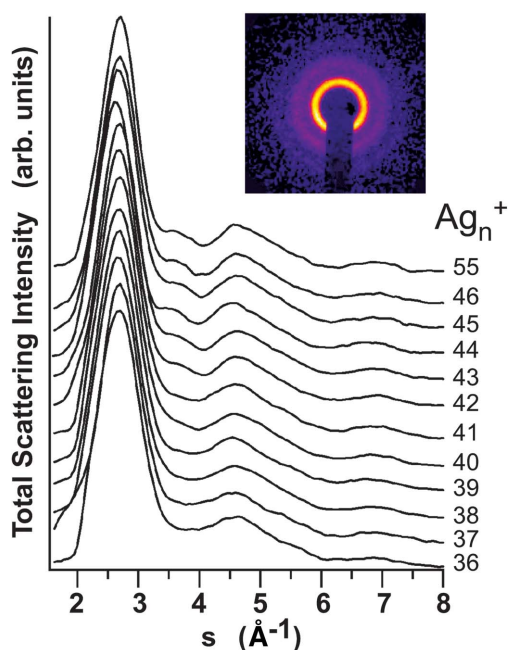


FIG. 1. (Color) Total scattering intensity vs s (\AA^{-1}) for Ag_n^+ cluster sizes $n=36-46, 55$. The inset is a colorized CCD image of the $n=55$ scattering pattern.

scattering factor, as shown in Fig. 2 for each cluster size studied. The diffraction data shown in Fig. 2 were obtained for unannealed clusters since no change was observed upon annealing, except for $n=38$ which is discussed below. Note in Fig. 2 that the peak positions and the positions on the s axis at which the data has zero values (zero crossings) are nearly identical for each cluster size, indicating that a similar symmetry is present at each cluster size. Each diffraction pattern in Fig. 2 displays the presence of fivefold symmetry as indicated by the shoulder on the second positive peak near $s \sim 5 \text{\AA}^{-1}$.^{11,12} The relative s values of the first two peaks $s_2/s_1=1.73 \pm 0.02$, and the location of the shoulder on the second peak, $s_{\text{sh}}/s_1=1.93 \pm 0.03$, are in good agreement with those expected for a perfect icosahedron,¹² $s_2/s_1=1.71$ and $s_{\text{sh}}/s_1=2.04$. The doublet structure in the first negative peak near $s \sim 3.8 \text{\AA}^{-1}$ is also characteristic of fivefold symmetry⁹ and is observed in Fig. 2 to become better resolved with increasing size. These changes in doublet structure can be shown analytically to arise from increased scattering interference as the fraction of Ag atoms having fivefold coordination increases.

Diffraction data were compared with theoretical calculations of cluster structures, performed for each cluster size $n=36-39, 43$, and 55 . In each case, a genetic algorithm¹³ and a many-body model potential¹⁴ were used to perform a

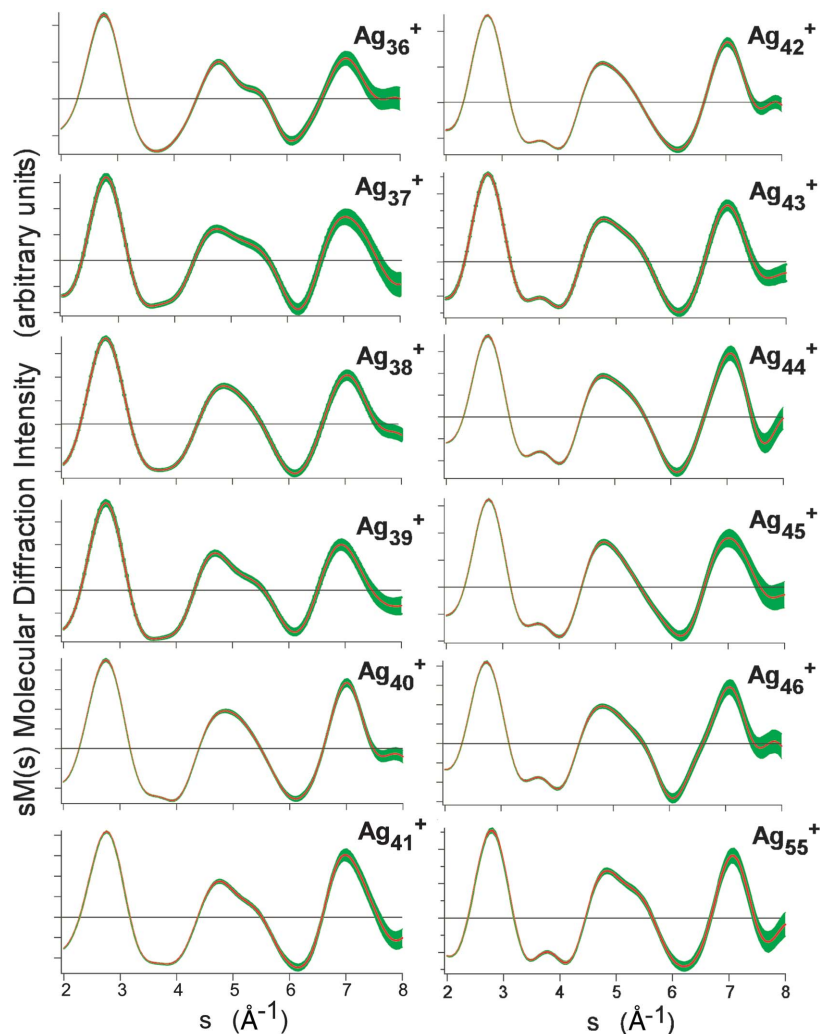


FIG. 2. (Color) Experimental molecular diffraction intensity $sM(s)$ vs s (\AA^{-1}) (red curve) for cluster sizes $n=36-46, 55$. The green shading shows the data uncertainty $\pm\sigma$.

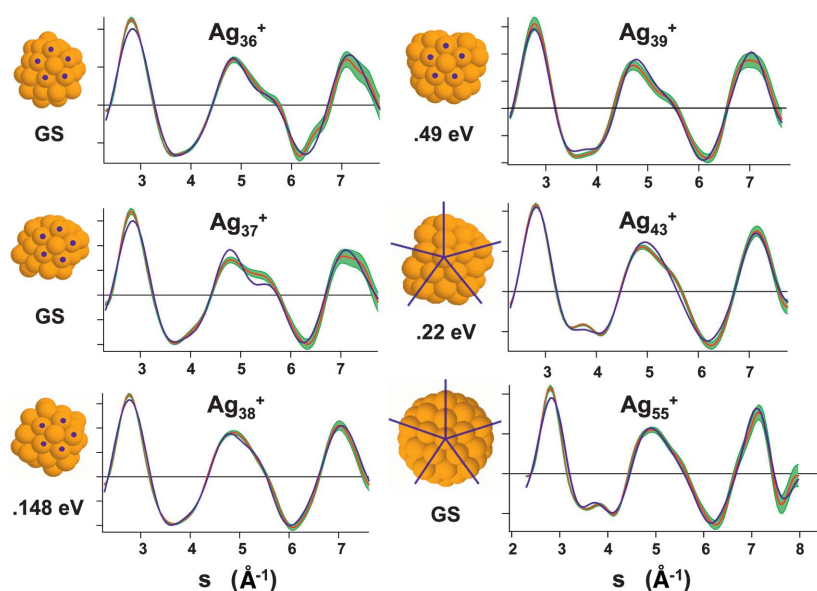


FIG. 3. (Color) Fits of experimental $sM(s)$ vs s (\AA^{-1}) (red curve) to theoretical models (blue curve) for cluster sizes $n=36-38$, 43, and 55. The green shading shows the data uncertainty $\pm\sigma$. The best fit isomer structure above the ground state (GS) are shown for each size. Areas of local order on the fit structures are indicated by blue dots, and blue lines indicate extended order, both of fivefold symmetry. The diffraction intensity has arbitrary units.

broad search of the structural phase space to identify an ensemble of the low energy isomers occurring with high frequency. The structures of $\sim 6-10$ lowest energy isomers corresponding to minima of the potential energy landscape were further optimized for the cationic clusters by generalized gradient approximation (GGA) density-functional calculations.¹⁵ These calculations identified only two cluster sizes, $n=38$ and 55, for which there was an isomer characterized by a global symmetry: truncated octahedral (fcc) at $n=38$ and icosahedral (Ih) at $n=55$, consistent with previous semiempirical calculations.^{16,17} The structures of all other isomers exhibited some degree of global asymmetry. To better characterize these isomers, the short-range order parameters $Q_{l,m}$ were calculated¹⁸ for each isomer structure. This parameter is formed from a set of spherical harmonics associated with every bond joining an atom to its nearest neighbors. The $Q_{l,m}$ for a given l value are averaged over bonds, squared and summed over m values to be invariant under rotation. The order parameter for $l=6$ is identified in Ref. 18 to indicate the importance of icosahedral symmetry and is used here as an objective measure of the icosahedral character of a cluster structure. The value $Q_6=0.104$ was calculated for the lowest energy isomer of $n=55$ which displayed global order having icosahedral symmetry. The value of Q_6 for 72% of all calculated isomers fell within a range of $\langle Q_6 \rangle = 0.13 \pm 0.03$, indicating the general presence of structures characterized by local order having fivefold symmetry. The value $Q_6=0.57$ found for the lowest energy isomer of $n=38$ is identical to the value calculated for fcc symmetry. However, the higher lying isomer of $n=38$ which agrees with the experimental results has $Q_6=0.11 \pm 0.01$, consistent with fivefold symmetry.

Vibrational effects were included in the theoretical structures by using the DFT structures to initialize molecular dynamics simulations¹⁹ at the experimental temperature of 120 K. An ensemble averaged diffraction pattern, $sM(s)$, for isomer was derived from the average of 10^3 atomic configurations extracted from these simulations. A theoretical model of the diffraction pattern was then composed of a sum of

isomer contributions representing an ensemble of trapped clusters composed of a mixture of isomer structures. The fitting procedure varied the fractional contribution of each isomer structure in the $sM(s)$ model to optimize the fit to experimental patterns. One of the more important elements of the fitting algorithm is a self-consistent determination of the independent scattering background contribution. The convergence of successive model fits for each isomer yields a refined background consistent with the optimum theoretical model. Performing these fits independently for each cluster size yields a set of background curves. It is important to point out that these background curves are expected to be very similar for all Ag cluster sizes aside from a normalizing factor. A master curve formed by averaging the individual background curves indicates the backgrounds were identical to within a standard deviation of $\pm 6\%$. This result ensures that the background extracted from each total scattering data set did not contribute to the evolving structure observed in the $sM(s)$ patterns.

The comparisons of diffraction data for unannealed clusters with theoretical models for each size are shown in Fig. 3. The fit uncertainty includes the standard deviations of the raw data and background added in quadrature. The quality of these fits indicate close agreement between the data and calculated structures, reinforcing the idea that the data evolves from cluster structures exhibiting local order having fivefold symmetry to a structure with global order having icosahedral symmetry as the cluster size increases.

There are several points to emphasize regarding these data fits. It is important to point out that only a single isomer made a significant contribution to the fits for sizes $n=36, 39, 43$, and 55. A marginally better fit was obtained for $n=37$ by including a second isomer contributing $\sim 30\%$ to the isomer mixture. Although the zero crossings and relative peak intensities are reproduced by the calculated structure, it is not clear why the calculated isomers only qualitatively describe the data obtained for Ag_{37}^+ in the region near $s=5 \text{\AA}^{-1}$. The rapid variation in this region is not observed in the data for any other cluster size, and it is possible that calculations have simply not identified the correct structure.

In the case of $n=38$, the truncated octahedron closed shell with fcc symmetry predicted as the lowest energy isomer for Ag_{38}^+ does not make any contribution to the unannealed diffraction data. Measurements were repeated for $n=38$ with annealing. The diffraction pattern for annealed Ag_{38}^+ continued to show no contribution from the isomer having fcc symmetry at energy 0.0 eV. However, the diffraction displayed a mixture of two isomer structures: the fivefold symmetry (40%) originally observed at energy 0.148 eV; and an isomer having slightly distorted decahedral symmetry (60%) at lower energy 0.064 eV. This is the only cluster size for which annealing made any significant difference in the diffraction data and emphasizes that cluster structures observed at finite temperature can exhibit effects of entropy and also kinetic relaxation on the potential energy surface.

The calculated structure for $n=43$ shown in Fig. 3 exhibits an ordered atomic arrangement similar to $n=55$ except for a relatively local region, and corresponds to the similarity observed in the 55 and 43 diffraction patterns observed in Fig. 2. At $n=55$, global order having icosahedral Ih symmetry is observed characterizing a closed shell structure. The global order observed for $n=55$ is consistent with a high symmetry structure indicated by photoelectron spectroscopy.²⁰

In summary, the present diffraction measurements have observed the structural evolution of Ag_n^+ in the range $n=36-55$. In the region $n < 55$, we have found that local order having fivefold symmetry dominates the cluster structures. With the exception of $n=38$, the Q_6 order parameters calcu-

lated for the isomers in Fig. 3, $\langle Q_6 \rangle = 0.11 \pm 0.01$, show negligible size dependence. This indicates that the number of local fivefold symmetry sites within these structures is increasing with size leading up to the closed atomic structure at $n=55$ having global order.

A question which motivates further measurements is whether the evolving Ag_n^+ structure simply derives from the closed shell Ih symmetry, or does local fivefold symmetry more generally characterize cluster structures evolving towards a global symmetry? We have conducted preliminary measurements of Au_n^- in the size range $n \leq 25$. These are observed to exhibit mixtures of isomer structures with local order having fivefold symmetry and tetrahedral Td (fcc) symmetry leading up to the closed shell pure Td at $n=20$.²¹ Investigations of disordered metal structures including metallic glasses and supercooled metal melts have observed^{11,22} and analyzed^{12,18} the presence of short-range order characterized by fivefold symmetry. Perhaps it is not surprising that these diffraction measurements have also observed such local symmetry in the structures of small metal clusters.

This work was sponsored by the Department of Energy under Grant No. DE-FG02-01ER45921. I.L.G. was supported by DGAPA-UNAM and Conacyt-Mexico under Project Nos. IN104402 and 43414-F, respectively. Fruitful discussions with F. Spaepen, O. Cheshnovsky, and L.S. Wang are acknowledged.

*Author to whom correspondence should be addressed. Electronic address: parks@rowland.harvard.edu

¹H. Haberland, T. Hippler, J. Donges, O. Kostko, M. Schmidt, and B. von Issendorff, *Phys. Rev. Lett.* **94**, 035701 (2005).

²C. L. Cleveland, W. D. Leudtke, and U. Landman, *Phys. Rev. Lett.* **81**, 2036 (1998).

³F. Furche, R. Ahlrichs, P. Weis, C. Jacob, S. Gilb, T. Bierweiler, and M. M. Kappes, *J. Chem. Phys.* **117**, 6982 (2002).

⁴H. Häkkinen, M. Moseler, and U. Landman, *Phys. Rev. Lett.* **89**, 033401 (2002).

⁵U. Heiz, A. Sanchez, S. Abbet, and W.-D. Schneider, *J. Am. Chem. Soc.* **121**, 3214 (1999).

⁶A. Sanchez, S. Abbet, U. Heiz, W.-D. Schneider, H. Häkkinen, R. N. Barnett, and U. Landman, *J. Phys. Chem. A* **103**, 9573 (1999).

⁷S. Krückeberg, D. Schooss, M. Maier-Borst, and J. H. Parks, *Phys. Rev. Lett.* **85**, 4494 (2000).

⁸J. H. Parks, in XII International Symposium on Small Particles and Inorganic Clusters Abstracts, Nanjing, China, September 2004 (unpublished); J. H. Parks, in Symposium on Size Selected Clusters Abstracts, Brand, Austria, February 2005 (unpublished).

⁹M. Maier-Borst, D. Cameron, M. Rokni, and J. H. Parks, *Phys. Rev. A* **59**, R3162 (1999).

¹⁰B. von Issendorff and H. Haberland, private communication.

¹¹K. F. Kelton, G. W. Lee, A. K. Gangopadhyay, R. W. Hyers, T. J. Rathz, J. R. Rogers, M. B. Robinson, and D. S. Robinson, *Phys. Rev. Lett.* **90**, 195504 (2005).

¹²S. Sachdev and D. R. Nelson, *Phys. Rev. Lett.* **53**, 1947 (1984).

¹³K. Michaelian, *Chem. Phys. Lett.* **293**, 202 (1998).

¹⁴V. Rosato, M. Guillope, and B. Legrand, *Philos. Mag. A* **59**, 321 (1989).

¹⁵E. M. Fernández, J. M. Soler, I. L. Garzón, and L. C. Balbás, *Phys. Rev. B* **70**, 165403 (2004).

¹⁶K. Michaelian, N. Rendón, and I. L. Garzón, *Phys. Rev. B* **60**, 2000 (1999).

¹⁷F. Baletto, A. Rapallo, G. Rossi, and R. Ferrando, *Phys. Rev. B* **69**, 235421 (2004).

¹⁸P. J. Steinhardt, D. R. Nelson, and M. Ronchetti, *Phys. Rev. B* **28**, 784 (1983); D. R. Nelson and F. Spaepen, in *Solid State Physics* (Academic Press, Boston, 1989), Vol. 42, p. 1.

¹⁹W. Zhong, Y. Cai, and D. Tománek, *Phys. Rev. B* **46**, 8099 (1992).

²⁰H. Häkkinen, M. Moseler, O. Kostko, N. Morgner, M. A. Hoffmann, and B. v. Issendorff, *Phys. Rev. Lett.* **93**, 093401 (2004).

²¹J. Li, X. Li, H.-J. Zhai, and L. S. Wang, *Science* **299**, 864 (2003).

²²T. Schenk, D. Holland-Moritz, V. Simonet, R. Bellissent, and D. M. Herlach, *Phys. Rev. Lett.* **89**, 075507 (2002).